Particle-cluster aggregation with dipolar interactions

R. Pastor-Satorras and J. M. Rubí

Departament de Física Fonamental, Facultat de Física, Universitat de Barcelona, Diagonal 647, 08028 Barcelona, Spain

The properties of aggregates generated from an off-lattice, two-dimensional, particle-cluster aggregation model with dipolar interparticle interactions have been investigated. The fractal dimension seems to be a monotonically decreasing function of the temperature, between a definite value close to 1 at $T = 0$ and the limit $T \to \infty$, corresponding to diffusion-limited aggregation of particles with no interaction. Temperature and dipolar interactions are introduced by means of a Metropolis algorithm. By analyzing the orientational correlation function, and what we call the orientation probability density of the direction of the dipoles on the clusters, an ordered state is found at low temperatures. This order diminishes when the temperature increases, due to the disorder induced by the fractal geometry of the aggregates. Our study is extended to the three-dimensional case. A disordered state is found even at $T = 0$, and a remnant order is shown when analyzing related two-dimensional correlations.

PACS number(s): 82.20.Wt, 61.43.Hv, 64.60.Cn

I. INTRODUCTION

The irreversible aggregation process of initially dispersed particles to form fractal clusters (i.e., fractal growth phenomena [1]) has attracted a great deal of interest in the last decade, especially since the development of computer models. There are two basic models of fractal aggregation: particle-cluster aggregation (PCA), the most well-known being the diffusion-limited aggregation (DLA) model of Witten and Sander [2], and cluster-cluster aggregation (CCA) [4,5]. In particular, numerical simulations performed with CCA models can describe the fractal structure of aerosols and colloids [3], which are in good agreement with experimental results. These computer models constitute coarse-grained simulations of the actual physical processes of aggregation, since they consider, in principle, a very simple short-ranged interparticle interaction: a hard-core, plus an infinite potential well on the surface of the particles, and no interactions for all other distances. For this reason, they are well-suited to simulate aggregation with interactions that strongly decay with distance, but they fail to describe aggregation with long-range interparticle forces.

Some authors have extended CCA and PCA models in order to take interparticle interactions into account. Ansell and Dickinson [6] proposed a CCA model in which particles experience hard-core plus van der Waals interactions by means of a Langevin dynamics algorithm. Meakin and Muthukumar [7,8] developed a model of reaction-limited CCA [9] with attractive and repulsive power-law interactions. On the other hand, Block *et al.* [10] presented a model of deterministic PCA, in which particles do not undergo a Brownian motion before being attached to the cluster. Instead, they undergo a deterministic trajectory under a power-law force exerted by the particles already incorporated in the cluster. A particularly interesting case is the aggregation of particles subject to dipolar forces, observed in ferrofluids and

the so-called magnetic holes [11]. Part of its interest lies in the simplicity of the experimental setup for its study, which can be easily performed with magnetized microspheres [12]. This kind of interaction has been simulated in a hierarchical CCA model [13] and in a box with periodic boundary conditions on its sides [14]. In this case, interactions are introduced by means of a Metropolis algorithm [15] and the results obtained are in close agreement with experience [14]. A hierarchical CCA model with ballistic trajectories [16] has also been proposed, yielding results that confirm those in Refs. [13,14]. However, because CCA simulations require a great amount of CPU time to generate large clusters, only modest-sized aggregates can be grown by means of these algorithms (up to 128 particles [13,14,16]). Those results do not allow categorical conclusions to be made about the fractal character of the dipolar clusters obtained.

Our purpose in this paper has been to extend the PCA model in order to include anisotropic dipolar interparticle interactions, by means of a Monte Carlo algorithm based on those described in Refs. [13,14]. Our algorithm is considerably faster than any other CCA dipolar model. At zero temperature, we have been able to generate clusters of up to 5000 particles in a reasonable amount of CPU time. For larger values of temperature, however, the CPU time needed to grow clusters containing more than 1000 particles is exceedingly large. In any case, we have achieved an increase in size of one order of magnitude, allowing an increased accuracy in the results and a reduction of statistical errors over previous studies. We have distributed the paper in the following way. In Sec. II, we describe our computer algorithm for the PCA of dipolar particles in two dimensions. Section III discusses some properties of these dipolar clusters. In particular, we compute the fractal dimension D as a function of temperature and study the order induced on the orientation of dipoles by its reciprocal interactions, which is reflected in two different kinds of orientational correlation functions. In Sec. IV we comment on the extension of our model

II. COMPUTER MODEL

In our two-dimensional (2D) off-lattice model, we consider the aggregation process of magnetic particles of diameter d and magnetic moment $\boldsymbol{\mu} = \mu \boldsymbol{u}$, with μ being the magnetic moment strength and $\boldsymbol{u}$ a unit vector oriented along its direction. The dipolar interaction between two particles i and j, located at the positions $\boldsymbol{r}_i$ and $\boldsymbol{r}_j$, respectively, is characterized by the energy

$$U_{ij} = \mu^2 u_{ij}, \qquad (2.1)$$

where u_{ij} is the dimensionless dipolar energy

$$u_{ij} = \left\{ \boldsymbol{u}_i \cdot \boldsymbol{u}_j - 3(\boldsymbol{u}_i \cdot \boldsymbol{r}_{ij})(\boldsymbol{u}_j \cdot \boldsymbol{r}_{ij})/r_{ij}^2 \right\} /r_{ij}^3, \qquad (2.2)$$

and $\boldsymbol{r}_{ij} = \boldsymbol{r}_i - \boldsymbol{r}_j$.

We start the simulation with a particle, referred to as the "seed," placed at the origin of coordinates, bearing a randomly oriented tridimensional vector $\boldsymbol{u}_1$, and parallel to the plane of growth. The following particles are released from a randomly chosen position on a circle of radius R_{in} centered on the seed. The released particles have assigned a vector $\boldsymbol{u}_i$ oriented at random. Each particle undergoes a random walk until it either contacts the cluster or moves away from the origin a distance greater than R_{out}. In this case, the particle is removed and a new one is launched from the circle surrounding the seed. Since magnetic dipole-dipole interactions are long range, the launching radius must be large enough in order to avoid bias in the shape of the cluster due to the initial conditions, i.e., the position on the launching circle where the particles were released. We have chosen the values $R_{\text{in}} = AR_{\text{max}} - \epsilon$ and $R_{\text{out}} = AR_{\text{max}}$, where R_{max} is the maximum radius of the cluster. The simulations have been carried out with the values $A = 2$ and $\epsilon = 5$, which are quite reasonable, due to the power-law decay of dipolar interactions. For $A = 2$, the energy decays on the average one order of magnitude from R_{max} (the neighborhood of the cluster) to R_{in} (the launching distance). A value of $A = 4$ has also been tested and it provides, within the error bars, the same result for the fractal dimension but the computation time increases dramatically.

The random walks experienced by the incoming particles are affected by the interactions exerted by the particles already attached to the cluster. We have taken this fact into account by using a Metropolis algorithm partially adapted from Refs. [13,14].

Suppose that the cluster is composed by $n-1$ particles, placed at the points $\boldsymbol{r}_i$, $i = 1, \ldots, n-1$. In some instant of time, the incoming nth random walker occupies the position $\boldsymbol{r}_n$ and its interaction with the already attached particles is given by the total energy

$$u_T = \sum_{i=1}^{n-1} u_{ni}. \qquad (2.3)$$

After a Monte Carlo time step, we compute a new position $\boldsymbol{r}'_n$ for the random walker. The particle arrives at this position by means of a Brownian motion, which occurs in a direction chosen at random and whose distance is one diameter d. The movement to the new position $\boldsymbol{r}'_n$ is performed rigidly, that is, the vector $\boldsymbol{u}_n$ does not change its orientation during the motion. The energy experienced in the new computed position $\boldsymbol{r}'_n$ is u'_T, and the total change in the energy due to the movement is $\Delta u_T = u'_T - u_T$. If $\Delta u_T < 0$, then the movement is accepted and performed. If $\Delta u_T > 0$, we compute the quantity

$$p = e^{-K \Delta u_T}, \qquad (2.4)$$

where parameter K determines the relative strength of the dipolar interaction versus the thermal energy and is given by

$$K = \frac{\mu^2}{d^3 k_B T}. \qquad (2.5)$$

($K^{-1} \sim T$ can be interpreted as some kind of dimensionless temperature, related to the intensity of the interaction.) In this latter case, the movement is performed with probability p. In the zero temperature limit, $K^{-1} = 0$, a movement is accepted if and only if it reduces the dipolar energy. In the high temperature limit, $K^{-1} \to \infty$, all movements are accepted: the particle undergoes a pure Brownian motion and we recover the classic DLA model. After every accepted movement, the moment of the random walker is relaxed, that is to say, it is oriented in the direction of the total field on its position. Indeed this fact assumes that the relaxation time for the orientation of particles is very short in comparison with the movement of the center of mass of the particles. The relaxation phenomenon will turn out to be crucial when analyzing the order of dipoles.

The particles stick to the cluster when they overlap one or more particles already incorporated to the aggregate. The new particle is then attached in the point of its last movement where it first contacted one of those particles. After sticking to the cluster, the new attached particle undergoes a last relaxation and its direction is not changed any more.

For $K^{-1} = 0$, this algorithm is quite fast. This is due to the fact that dipolar interactions attract the incoming particles towards the cluster, avoiding time-consuming spurious movements far from it. In this case, it is possible to grow clusters up to 5000 particles in a reasonable amount of CPU time. For $K^{-1} \geq 10^{-3}$, the algorithm becomes very slow, because of the predominance of thermal disorder over magnetic attraction in the Brownian motion. A cluster of 1000 particles at a temperature $K^{-1} = 10$ (the greatest simulated) requires about 8–10 h of CPU time on an Apollo 9000/730 workstation; a cluster of 1500 particle may take more than a week of CPU time. We have generated and analyzed about 150 clusters containing 1000 particles, for different values of K^{-1} ranging from 0 to 10; for each value a number between 10 and 40 of aggregates have been simulated. Figure 1 shows some typical clusters of 1000 particles correspond-
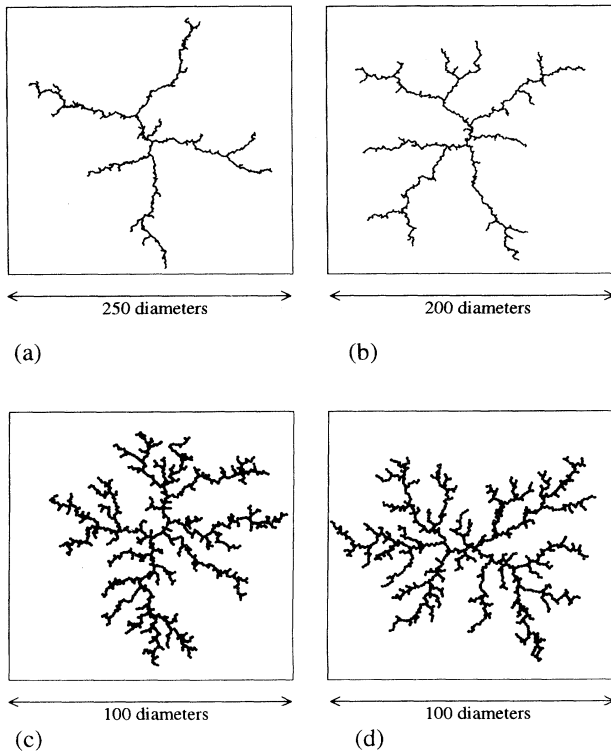
FIG. 1. Typical 2D dipolar clusters of 1000 particles, generated for several values of K^{-1}. (a) $K^{-1} = 0$, $D = 1.20 \pm 0.02$. (b) $K^{-1} = 10^{-3}$, $D = 1.35 \pm 0.04$. (c) $K^{-1} = 10$, $D = 1.74 \pm 0.02$. (c) Pure DLA cluster, grown in the limit $K^{-1} \to \infty$, $D = 1.71 \pm 0.01$.

ing to four different values of K^{-1}. In order to detect finite-size effects, we have also generated 10 clusters at $K^{-1} = 0$ containing 5000 particles, the largest cluster size available with our computer resources.

III. RESULTS

A. Fractal dimension

The fractal dimension D is determined from a log-log plot of the radius of gyration of the cluster

$$R_g(N) = \left(\frac{1}{N} \sum_{i=1}^{N} (r_i - r_{\text{c.m.}})^2 \right)^{1/2} \tag{3.1}$$

as a function of the number of particles N (see, for example, Ref. [1]). From the relationship $R_g(N) \sim N^\nu$, we get $D = 1/\nu$. The exponent ν is computed by a least-squares fitting of $\log(R_g(N))$ on $\log(N)$ (all logarithms in this paper are in base 10) for each aggregate, and the different values are averaged over the ensemble of clusters generated for the same value of K^{-1}.

In order to check our algorithm, we have generated 100 clusters containing 1000 particles in the limit $K^{-1} \to \infty$ (true DLA with no dipolar interactions). In this case, the moment of each particle was randomly oriented. The fractal dimension computed is $D = 1.71 \pm 0.01$ (statistical

errors in this paper are at a 95% confidence limit). We thus recover, within the error bars, the well-known value $D = 1.715 \pm 0.004$ [17].

The fractal dimension D has been computed for the aggregates grown at each analyzed value of K^{-1}. Some remarkable results are in order.

(i) $K^{-1} = 0$. For 10 clusters of 5000 particles, we get a fractal dimension $D = 1.13 \pm 0.01$, whereas for 40 clusters of 1000 particles, $D = 1.20 \pm 0.02$. We can explain this discrepancy by analyzing D as a function of N for the clusters containing 5000 particles, Fig. 2. We notice that D establishes itself on a value around 1.13 for $N > 3000$, whereas for $N < 3000$ its value fluctuates and is somewhat larger. At $K^{-1} = 0$, a cluster of 1000 particles has not yet reached a stable state and the fractal dimension we compute from it is slightly overestimated. This is also true for the smaller values of K^{-1} simulated. In any case, the value of D is clearly lower than the one corresponding to true DLA. In Fig. 1(a) we can see a typical cluster with dipolar interactions grown at $K^{-1} = 0$. We can compare the form of this aggregate with the one corresponding to true DLA, grown with the same algorithm, which is shown in Fig. 1(d). The dipolar cluster has a much lesser branched and a more open structure, that is to say, it has a smaller *bifurcation ratio* [18].

(ii) $K^{-1} = 10^{-3}$. In the cluster-cluster aggregation experiment described in Ref. [14], magnetic particles were employed for which $K \simeq 1360$, at room temperature. In our simulations, the fractal dimension obtained for clusters grown at $K^{-1} = 10^{-3}$ is $D = 1.35 \pm 0.04$. Figure 1(b) shows a typical cluster of this kind. This value of D is clearly different, out of the error bars, from that computed for $K^{-1} = 0$.

(iii) $K^{-1} = 10$. For this value of K^{-1}, which is the largest we have considered, we find $D = 1.74 \pm 0.02$.
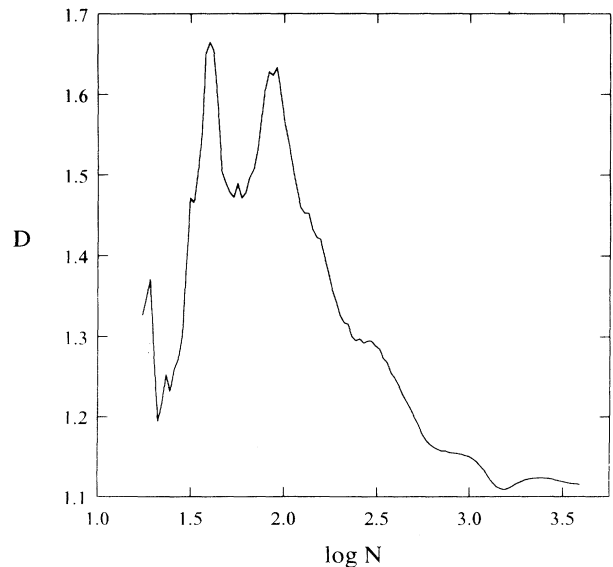

FIG. 2. Fractal dimension D as a function of N for 2D dipolar clusters grown at $K^{-1} = 0$. The values of D have been computed at several stages of the growth of the clusters. The logarithm is to the base 10 here and throughout.

Figure 1(c) shows a typical cluster at $K^{-1} = 10$. The fractal dimension has already reached, within the error bars, the limit value of true DLA $(K^{-1} \to \infty)$.

Figure 3 shows a plot of D as a function of K^{-1} for the whole range of values analyzed. It seems to exhibit a *smooth* increasing behavior when increasing K^{-1}, the values of D ranging between the limits corresponding to $K^{-1} = 0$ (aggregation with dipolar forces of infinite strength or zero temperature) and $K^{-1} = \infty$ (aggregation with no interactions or infinite temperature).

In order to understand this situation we can provide a theoretical reasoning. Let us consider a particle that is going to be attached to the cluster, onto another one belonging to the cluster. It can stick on the *tip* of a branch with probability P_g, thus contributing to its growth, or it can do so *along* the branch with probability P_s and, therefore, contribute to its splitting. Both probabilities are related to the dipolar forces and thermal disorder (Brownian motion) through the so-called *growth-site probability distribution* [1]. Since dipolar interactions decay as r^{-3}, we can consider that the main contribution to the energy comes from the interaction between the incoming particle and the particle on the cluster on which the new one is going to be attached. Given the expression (2.2) for the energy, we have two possible positions energetically favored, depicted in Fig. 4, which minimize u_{ij}. Due to the relaxation mechanism, position 4(a) can only happen on the tip of a branch, and therefore it is related to the *growth* of the branch and to the growing probability P_g. Position 4(b), on the other hand, can occur along the whole branch, being related to *splitting* and to the splitting probability P_s. These probabilities are given by the energy of their respective configurations, $u_g = -2$ and $u_s = -1$, through a Boltzmann factor. Then one has
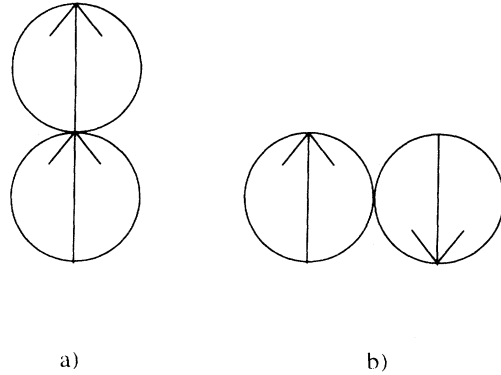

a)   b)

FIG. 4. Given the expression (2.2), there are two possible relative positions which minimize dipolar energy. Position (a), associated with the growth of a given branch (energy $u_g = -2$), and position (b), associated with its split (energy $u_s = -1$).

$$\frac{P_g}{P_s} \sim \exp\left[-K(u_g - u_s)\right] = \exp(K), \qquad (3.2)$$

where u_g and u_s are the energies of the two configurations.

At zero temperature, $K \to \infty$, we have $P_s = 0$; the most likely event is the growth of a given branch, not its split. Neglecting the effect of thermal disorder, we should then expect at $K^{-1} = 0$ an aggregate of $D = 1$. In fact, Fig. 2 hints in this direction. $D(N)$ seems to be a decreasing function of N and we cannot reject the possibility of $D \to 1$ in the limit $N \to \infty$. The actual finite branching found in our simulations at $K^{-1} = 0$ is due to the randomness introduced by the Monte Carlo algorithm, which tends to be negligible in the limit of large cluster sizes. For large values of K^{-1}, we have $P_g \sim P_s$; the growth of a given branch and its split are equally likely events. The effect of dipolar interactions is overcome by the Brownian disorder and we recover the original DLA model with no interactions. At intermediate values of K, the ratio between growing and splitting probabilities given by dipolar interactions evolves continuously, as well as the effect of thermal disorder. We should expect a continuous change in the geometry of the cluster and, therefore, a smooth dependence of D on the temperature.

B. Correlation functions

Dipolar interactions, by means of the magnetic relaxation procedure, induce a microscopic order in the orientation of magnetic moments. Neighbor dipoles cannot point in random directions but must be correlated, the orientation of each one being given by the total magnetic field generated by the cluster at the point where the particle was attached. In Fig. 5 we have drawn the orientation of the dipoles associated with the particles belonging to the inner region around the seed, for the clusters shown in Fig. 1. As we can see, dipoles belonging to the same
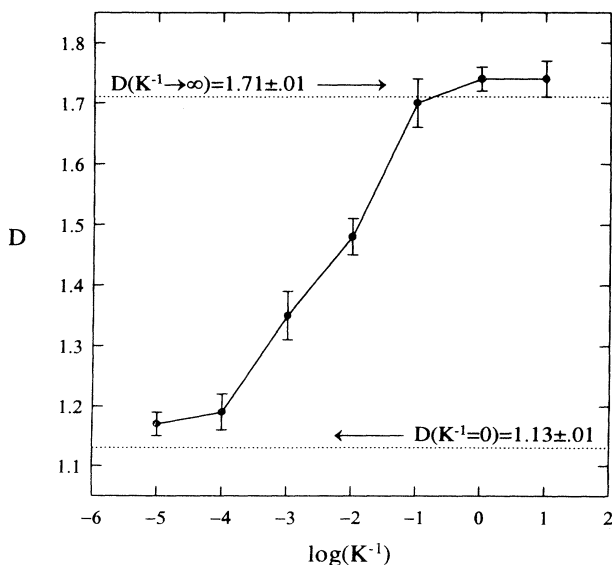

FIG. 3. Fractal dimension D as a function of K^{-1} for 2D dipolar clusters.

neighborhood point in the direction of the local field on its position, for any value of K^{-1}.

One way of obtaining information about the orientation order in the cluster is to study the correlations between the moments of its particles. Following Ref. [19], we define in 2D the ordinary *density-density* or *pair correlation function*

$$g_0(r) = (2\pi r \Delta r N)^{-1} \sum_{r - \frac{\Delta r}{2} < |\mathbf{r}' - \mathbf{r}''| < r + \frac{\Delta r}{2}} \rho(\mathbf{r}')\rho(\mathbf{r}''),$$

$$(3.3)$$

where $\rho(\mathbf{r})$ is equal to 1 if a particle occupies the position $\mathbf{r}$ and 0 otherwise. Δr is the length step in a space discretization. For fractal aggregates, the pair correlation function exhibits a power-law behavior, with

$$g_0(r) \sim r^{-\alpha}, \qquad (3.4)$$

the fractal dimension being given by $D_\alpha = d_E - \alpha$ (correlation dimension). In this case, $d_E = 2$ is the Euclidean dimension of the embedding space.

Following [19], we can define a *vector correlation function* depending on the *relative orientation* of pairs of dipoles separated a distance r,

25 diameters   25 diameters

(a)   (b)

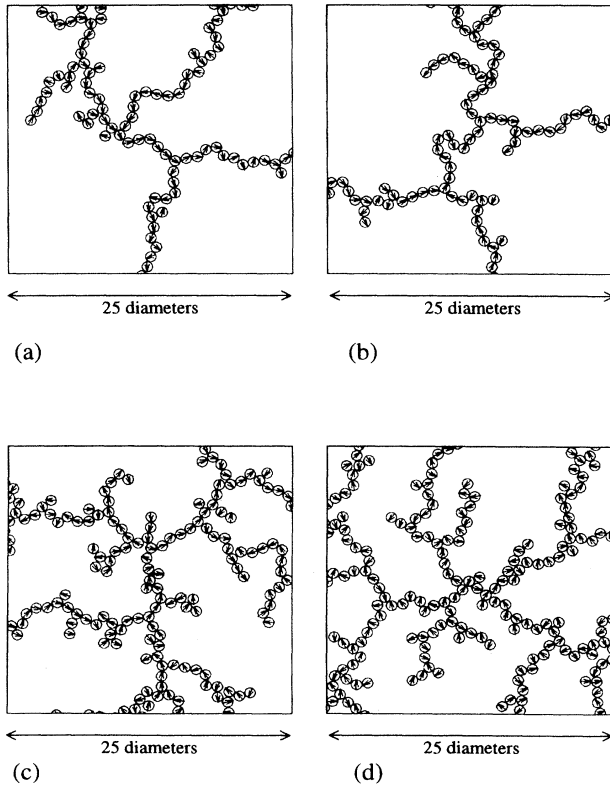25 diameters   25 diameters

(c)   (d)

FIG. 5. Close up of the inner regions around the seed of the clusters shown in Fig. 1. The dipoles attached to each particle have been drawn in order to compare their relative orientations. (a) $K^{-1} = 0$. (b) $K^{-1} = 10^{-3}$. (c) $K^{-1} = 10$. (d) Free DLA cluster ($K^{-1} \to \infty$). The orientation of its dipoles has been assigned at random.

$$g_1(r) = (2\pi r \Delta r N)^{-1} \sum_{r - \frac{\Delta r}{2} < |\mathbf{r}' - \mathbf{r}''| < r + \frac{\Delta r}{2}} \mathbf{u}(\mathbf{r}') \cdot \mathbf{u}(\mathbf{r}''),$$

$$(3.5)$$

where $\mathbf{u}(\mathbf{r})$ is the unit vector oriented along the direction of the magnetic moment of the particle located at position $\mathbf{r}$. This function is a quantitative measure of orientational correlations between pairs of dipoles. We can also define another correlation function of the moments of a cluster

$$g_2(r) = (2\pi r \Delta r N)^{-1} \sum_{r - \frac{\Delta r}{2} < |\mathbf{r}' - \mathbf{r}''| < r + \frac{\Delta r}{2}} |\mathbf{u}(\mathbf{r}') \cdot \mathbf{u}(\mathbf{r}'')|,$$

$$(3.6)$$

which depends on the *absolute value* of the scalar product of pairs of moments. Due to the fractal nature of the clusters, we expect a scaling behavior for these functions [19], $g_1(r) \sim r^{-\alpha_1}$ and $g_2(r) \sim r^{-\alpha_2}$, and also the same scaling exponent for $g_2(r)$ as for the pair correlation function $\alpha_2 = \alpha$.

Figure 6 shows a log-log plot of the correlation functions $g_0(r)$, $g_1(r)$, and $g_2(r)$ computed from 10 clusters generated at $K^{-1} = 0$, and composed of 5000 particles. All three functions exhibit a power-law behavior with r. From the plot of $g_0(r)$ we compute the exponent $\alpha = 0.82$, which provides a fractal dimension $D_\alpha = 1.18$, quite similar to the value obtained from the radius-of-gyration method ($D = 1.13$). As expected, the vector correlation function $g_2(r)$ decays with the same exponent as the pair correlation function, $\alpha_2 = \alpha = 0.82$, whereas $g_1(r)$ scales with a different exponent, $\alpha_1 = 1.00$. The
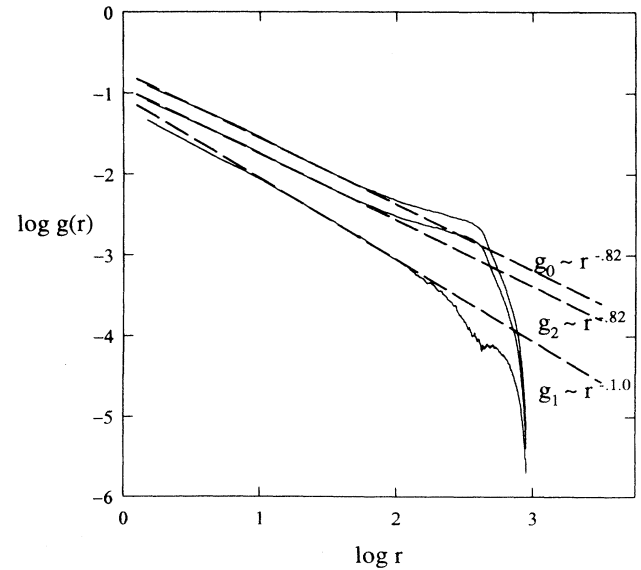

log r

FIG. 6. Correlation functions $g_0(r)$, $g_1(r)$, and $g_2(r)$, computed from 10 2D clusters grown at $K^{-1} = 0$ and containing 5000 particles. All three functions present power-law behavior, with the same exponent 0.82 for $g_0(r)$ and $g_2(r)$, and a different exponent, close to 1.0, for $g_1(r)$.

vector correlations for dipole orientations show a behavior similar to the correlations for bond vectors described in Ref. [19]. As was found in that paper, $g_1(r)$ scales with a different exponent from $g_0(r)$. However, the difference between the exponents we have found is not as dramatic as it was in the case discussed in [19].

We have also computed the correlation functions from the ensembles of clusters composed of 1000 particles grown at different values of K^{-1}. From our results we conclude that $g_2(r)$ always exhibits the same scaling exponent as the pair correlation function. Figure 7 shows the functions $g_1(r)$ computed in a range of values of K^{-1} between 0 and 10^{-2}. These correlations seem to present a power-law behavior with an exponent $\alpha_1 \sim 1$, roughly independent of K^{-1}. Figure 8 shows $g_1(r)$ computed from clusters in the range of K^{-1} between 10^{-1} and 10. In order to compare the behavior of these functions with a limit case of maximum disorder, we have also plotted in this figure the vector correlations computed from two ensembles of 25 pure DLA clusters (grown with no interactions), each one composed of 5000 particles. The particles of these aggregates have attached dipoles with orientations assigned in two different ways. For the first ensemble, we assign *relaxed dipoles*: the seed of the cluster bears a dipole pointing in a randomly chosen direction; the orientation of the particles successively added to the cluster is chosen to be parallel to the total magnetic field in the point where the particle was attached. For the second ensemble, we assign *random dipoles*: the dipole orientation of each particle is chosen completely at random. DLA with relaxed dipoles can be interpreted as the limit case of growth at $K^{-1} \to \infty$ with dipolar interactions whose only effect is to relax the vector dipoles in the direction of the total magnetic field. DLA with random dipoles can be seen as the limit case of growth

FIG. 8. Vector correlation functions $g_1(r)$ computed from several ensembles of 2D dipolar 1000-particle clusters in a range of values of K^{-1} between 10^{-1} and 10, and from two ensembles of 25 5000-particle 2D DLA clusters. The particles in these latter ensembles have attached relaxed and randomly oriented dipoles, respectively (see text). The vector correlations are short-ranged, with a limit in a maximal disorder situation, DLA with random dipoles. We have used a semilogrithmic plot due to the nonpositive character of $g_1(r)$.

with no dipolar interactions, and thus with no ordering effects at all.

In all the cases shown in Fig. 8, $g_1(r)$ is not a positive definite function. That is to say, for any value of K^{-1} greater than 10^{-2}, the vector correlations are no longer long range (power law). Correlations tend to decrease when increasing the temperature towards a well-defined limit at $K^{-1} \to \infty$ (DLA with relaxed dipoles), in which we found a remnant order due to the relaxations mechanism. When interactions are completely removed (DLA with random dipoles) there is no order left.

These results can be interpreted as follows. For small values of the temperature $(K^{-1} \to 0)$, the relaxation procedure produces a microscopic order in the orientation of dipoles (on neighbor dipoles) which induces a macroscopic correlation of orientations over long distances, thus yielding a long-range behavior pattern for the vector correlations. For large values of the temperature $(K^{-1} \to \infty)$, thermal disorder prevails, through the fractal geometry of the aggregates, over relaxational order and the vector correlations become short range: dipoles are uncorrelated over long distances. As we can see from Figs. 7 and 8, the vector correlations change continuously with K^{-1}; the order induced by relaxation is smoothly affected by the changes in the geometry of the cluster produced by increasing thermal disorder. Therefore, we can conclude that the changes in the geometry with temperature must also be continuous, and the same should be true for the fractal dimension. Because of the sudden change in the behavior of $g_1(r)$ from long to short range, however, we cannot exclude the possibil-
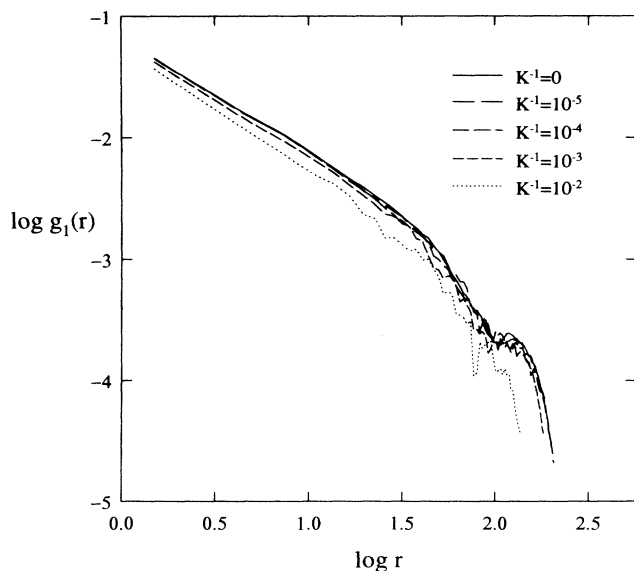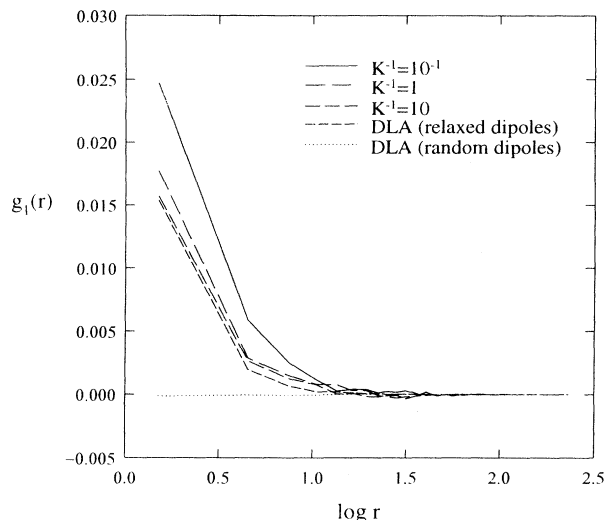

FIG. 7. Vector correlation functions $g_1(r)$ computed from several ensembles of 2D dipolar clusters in a range of values of K^{-1} between 0 and 10^{-2}. All of them exhibit a power-law behavior with roughly the same scaling exponent $\alpha_1 \simeq 1$.

ity of a crossover, with a sharp fall of D for some value K_c^{-1} around 10^{-2}, a fall that we have not detected in our simulations because of the limited size of the clusters we have generated.

C. Orientation probability density

Another direct way to measure correlations between pairs of dipoles is simply to study its *relative orientation*. Consider a pair of dipoles in a cluster whose directions form a certain relative angle θ, which we consider normalized to the interval $[0, \pi]$. We introduce a new quantity, the *orientation probability density* (OPD) $P(K, \theta)$, which we define as follows: $P(K, \theta)d\theta$ is the probability that the angle formed by the directions of a pair of dipoles, chosen at random from a cluster generated at some given value of K, is included in the interval $[\theta, \theta + d\theta]$.

This probability density is a measure of the order of the dipoles on the cluster. In a completely disordered distribution, all relative orientations are equally probable and, therefore, we have $P(\theta) = \text{const} = \frac{1}{\pi}$. In a distribution in which all the dipoles point in the same direction, every pair forms a relative angle of zero radians, then $P(\theta) = \delta(\theta)$. A given distribution of dipoles will provide some density $P(K, \theta)$ between these two limit values.

In order to determine $P(K, \theta)$, we fix a small angular increment $\Delta\theta$. On the set of all pairs of dipoles in a cluster (generated at some given value of K^{-1} and composed of N particles), we compute the function $n(K, \theta)$, which is defined as the number of pairs with a relative angle between θ and $\theta + \Delta\theta$. We then have

$$P(K, \theta) = \frac{2}{N(N-1)} \frac{1}{\Delta\theta} n(K, \theta). \qquad (3.7)$$

In order to reduce statistical uncertainties, these values are averaged over the ensemble of clusters grown at the same temperature.

Figure 9 shows $P(K, \theta)$ computed from several ensembles of clusters of 1000 particles, grown at different values of K^{-1}, between 0 and 10. For small values of K^{-1} $(K^{-1} \leq 10^{-2})$ we can fit $P(K, \theta)$ to the function

$$P(K, \theta) = a(K) + b(K)\cos\theta. \qquad (3.8)$$

This function must be normalized such that

$$\int_0^\pi P(K, \theta)d\theta = \pi a(K) = 1, \qquad (3.9)$$

which implies that $a(K) = \pi^{-1}$. A least-squares fitting of $P(K, \theta)$ on $\cos\theta$ provides the values for the coefficients $a(K)$ and $b(K)$ given in Table I. As expected, the coefficients $a(K)$ are almost independent of K^{-1} and its average over the range of values of K^{-1} is $\langle a \rangle^{-1} = 3.153 \pm 0.002$, quite similar to the predicted value π.

For values of $K^{-1} > 10^{-2}$, $P(K, \theta)$ is almost constant: $P(K, \theta) = a'(K)$, with $a'(K) = \pi^{-1}$. A least-squares fitting of $P(K, \theta)$ on $\cos\theta$ and θ provides in both cases poor values for the goodness-of-fit correlation coefficients. The coefficient $a'(K)$ is now obtained by averaging the
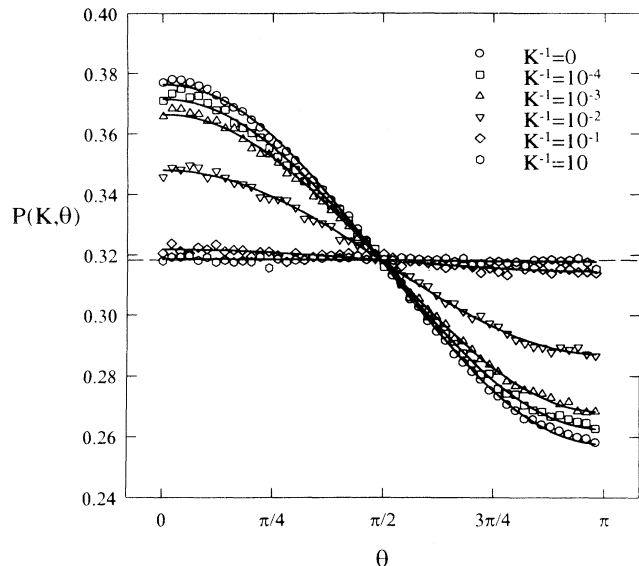

FIG. 9. Orientation probability density $P(K, \theta)$ computed from several ensembles of 2D dipolar clusters composed of 1000 particles, at different values of K^{-1}. For small values of K^{-1}, $P(K, \theta)$ exhibits a sinusoidal behavior; for larger values of K^{-1}, this function is almost constant, which is evidence of a significant orientational disorder. Solid lines are least-squares fittings.

function $P(K, \theta)$ on its range of discretized angles, θ_i, $i = 1, \ldots, n$,

$$a'(K) = \frac{1}{n} \sum_{i=1}^n P(K, \theta_i). \qquad (3.10)$$

The computed values are given in Table II, and the corresponding average is now $\langle a' \rangle^{-1} = 3.142 \pm 0.001$.

As we can see from our results, $P(K, \theta)$ can be fitted to the functional form (3.8) for the whole range of K values. The coefficient $a(K)$ is the normalization constant $(a(K) = \pi^{-1})$. The coefficient, which measures the strength of the correlations, is a decreasing function of K^{-1}; that is, the correlations of relative orientations tend to diminish when increasing the temperature (thermal disorder) towards the limit value $b = 0$. The limit is already reached for $K^{-1} > 10^{-2}$.

The OPD $P(K, \theta)$ presents quite similar behavior as the vector correlation function $g_1(r)$. In the low temperature limit, the orientation of the dipoles is strongly

TABLE I. Coefficients of a least-squares fitting on $a(K) + b(K)\cos\theta$ for the OPD of 2D dipolar clusters grown at given values of K^{-1}.

K^{-1}	a (K)	b (K)
0	0.3170 ± 0.0003	0.0594 ± 0.0005
10^{-5}	0.3171 ± 0.0004	0.0585 ± 0.0006
10^{-4}	0.3171 ± 0.0004	0.0545 ± 0.0006
10^{-3}	0.3172 ± 0.0004	0.0492 ± 0.0005
10^{-2}	0.3176 ± 0.0004	0.0305 ± 0.0005

TABLE II. Average value of the OPD of 2D dipolar clusters grown at given values of K^{-1}.

K^{-1}	a' (K)
10^{-1}	0.3182 ± 0.0004
1	0.3182 ± 0.0004
10	0.3182 ± 0.0003

correlated, and this yields a sinusoidal behavior for the orientation density. As the temperature rises, the OPD decreases continuously. In the high temperature limit, the dipoles show a great deal of disorder (imposed by the disorder of its intrinsic fractal geometry) and the OPD is almost constant (all relative orientations are equally probable). This latter point has been checked by computing the function $P(K, \theta)$ from two ensembles of 25 DLA clusters composed of 5000 particles with relaxed and random attached dipoles, respectively. In both cases the orientation density is almost constant, with an average value $\langle a' \rangle^{-1} = 3.143$. Once again, the continuous variation of the OPD hints toward a smooth dependence of the geometry on the temperature and, consistently, toward a continuous dependence of the fractal dimension on K^{-1}.

IV. 3D MODEL

Our 2D computer model can be easily extended to the three-dimensional (3D) case. The parameters A and ϵ for the launching and killing radius defined in Sec. II have to be carefully chosen now in order to avoid bias in the shape of the clusters and allow reasonable execution CPU times. For $K^{-1} = 0$, and due to the attractive forces exerted by the cluster on the incoming particles, the same values as in the 2D case, namely $A = 2$ and $\epsilon = 5$, were employed. Because of limitations in our computer resources, we have only generated clusters of a maximum radius of $75d$. This fact imposes an upper limit on the maximum number of particles allowed in a cluster.

In order to check our algorithm, we have grown 10 3D DLA clusters (without dipolar interactions) containing 10 000 particles. The radius-of-gyration method yields a fractal dimension $D = 2.46 \pm 0.04$, in close agreement within the error bars, with the known value $D = 2.495 \pm 0.005$ [17].

We have generated 30 3D dipolar clusters composed of 1000 particles at $K^{-1} = 0$. Figure 10 shows the perpendicular projections over the coordinate planes for a typical 3D dipolar cluster. The fractal dimension computed from this ensemble is $D = 1.37 \pm 0.03$, a smaller value than for noninteracting 3D DLA clusters.

The different correlation functions considered in Sec. III B for the 2D case have also been computed from these clusters. These correlation functions correspond to the ones introduced through Eqs. (3.3), (3.5), and (3.6), but with the normalization factor $\left(4\pi r^2 \Delta r N\right)^{-1}$, corresponding to a 3D space.

As a result, we have found that the correlations $g_0(r)$
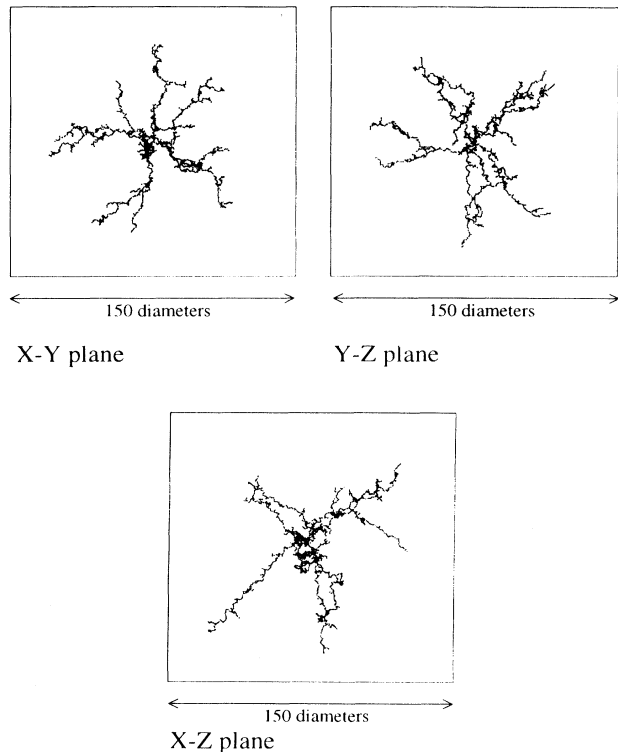

X-Y plane Y-Z plane

X-Z plane

FIG. 10. Perpendicular projections over the coordinate planes for a typical 3D dipolar cluster composed of 1444 particles, grown at $K^{-1} = 0$, $D = 1.37 \pm 0.03$.

and $g_2(r)$ present a scaling behavior with the same exponent as in the case 2D, whereas the vector correlation function $g_1(r)$ is a nonpositive definite function, which exhibits the short-range behavior of vector correlations in a 3D space.

The OPD for 3D dipolar clusters $P(\theta)$ can also be computed by means of expression (3.7). The relative angle θ in 3D is now the azimuthal angle in spherical coordinates on a relative frame of reference. Figure 11 shows $P(\theta)$ for the ensemble of dipolar clusters, together with the orientation density computed from two ensembles of 3D DLA clusters of 10 000 particles, which have assigned relaxed and random dipoles, respectively. All three functions can be fitted to the expression $P(\theta) = \frac{1}{2}\sin\theta$, which is the density of an equiprobable distribution of azimuthal angles in 3D spherical coordinates. That is to say, in a 3D space the relative orientation of dipoles at zero temperature is randomly distributed.

This fact contrasts with the relative order induced by relaxation in 2D. In order to explore this effect, we have computed the function $P'(\theta)$, defined as the orientation probability density for the *normalized bidimensional projections of the components of the 3D dipoles over the X-Y plane*. If e_α stands for an orthonormal base for the X-Y plane, the normalized projection $\hat{u}$ of the vector u is given by

$$\hat{u} = \frac{1}{\left|\sum_\alpha (e_\alpha \cdot u)e_\alpha\right|} \sum_\alpha (e_\alpha \cdot u)e_\alpha. \qquad (4.1)$$
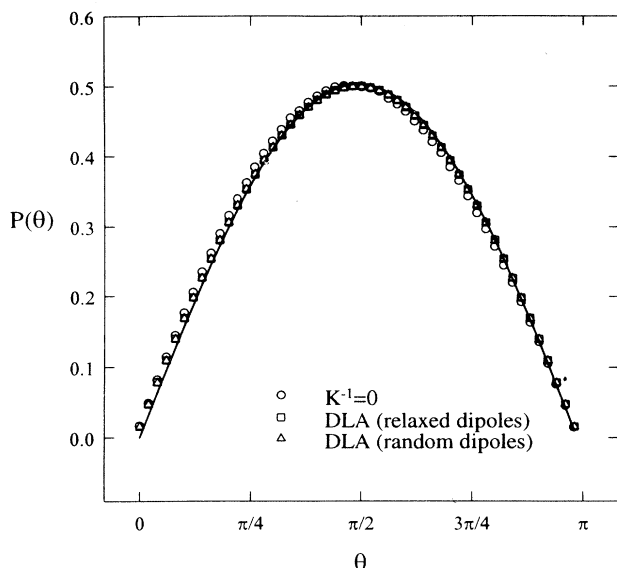
FIG. 11. Orientation probability density $P(\theta)$ computed from 3D dipolar clusters and DLA clusters with relaxed and randomly oriented dipoles. The three distributions can be fitted to the function $\frac{1}{2}\sin\theta$ (solid line), which corresponds to an equiprobable distribution of azimuthal angles in 3D spherical coordinates. Dipole relative orientation presents, therefore, a maximum disorder.

FIG. 12. Orientation probability density for the normalized projections of 3D dipoles over the X-Y plane, $P'(\theta)$, computed from 3D dipolar clusters and DLA clusters with relaxed and randomly oriented dipoles. The density for 3D dipolar clusters can be fitted to the function $P'(\theta) = 0.32 + 0.0087\cos\theta$ (solid line). We thus recover the sinusoidal behavior shown in 2D, while for the DLA cluster the projected dipoles still present a maximum disorder.

It has no meaning to compute the vector correlation functions of the normalized projections, because they do not have a well-defined minimum cutoff distance (particle diameter in the original 3D space).

Figure 12 shows $P'(\theta)$ computed from the ensemble of 3D dipolar clusters at $K^{-1} = 0$, and from two ensembles of 3D DLA clusters with relaxed and randomly oriented dipoles. For the DLA clusters, the OPD of the projected dipoles is almost constant, corresponding to a maximum disorder. However, for dipolar clusters it shows a clear sinusoidal behavior, as it was the case in 2D growth. A least-squares fitting on $\cos\theta$ provides the expression $P'(\theta) = 0.32 + 0.0087\cos\theta$. In 3D the dipolar interaction induces some kind of underlying order in the dipole orientations, which only becomes apparent in analyzing the bidimensional properties of the clusters.

V. CONCLUSIONS

In this paper we have investigated the effects of dipolar interparticle interactions in particle-cluster aggregation in two and three dimensions. The fundamental parameter turns out to be the dimensionless magnitude K^{-1}, Eq. (2.5), which is related to the temperature of system T and to the relative strength of the magnetic interactions μ. In 2D our results are summarized as follows.

(i) For $K^{-1} = 0$ (low temperature, strong magnetic forces), clusters are formed with a small value of the fractal dimension $D = 1.13 \pm 0.01$. The aggregates have a less branched and more open structure than DLA with no interactions. This fact can be explained as the effect
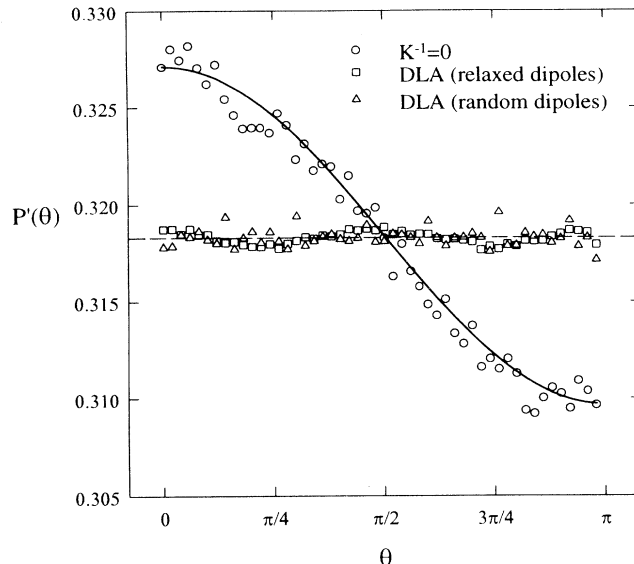
of dipolar forces over the growth-site probability distribution of the clusters [1]. The growth of a given branch is much more likely than its split, which results in an enhancement of the screening of the aggregate's inner regions.

(ii) When increasing K^{-1} (high temperature, weak magnetic forces), we recover a result already found in previous works [13,14,16]: the fractal dimension raises its value until it reaches the limit value of DLA with no interactions. The plot of D as a function of K^{-1}, Fig. 3, seems to show quite smooth and continuous behavior. This fact can be explained by a continuous relative increment of the splitting probability P_s over the growing probability P_g when increasing the temperature, which would cause a rise in the bifurcation ratio and therefore a rise in the fractal dimension. Nevertheless, we cannot utterly reject the possibility of a crossover, with a sharp fall of D at some definite value of K^{-1}. In order to check this possibility, larger clusters must be generated for intermediate values of K^{-1}.

(iii) The short relaxation time for the orientation of dipoles, implemented in our model through the relaxation mechanism discussed, induces a microscopic order in the orientation of neighbor dipoles. At low temperature $(K^{-1} \leq 10^{-2})$, this microscopic order induces a macroscopic ordering in the whole cluster, which is revealed by two kinds of measurements: (1) the vector correlation function (3.5) shows a power-law behavior (long-range correlations) with a scaling exponent $\alpha_1 = 1.0$ roughly independent of K^{-1}; (2) the orientation probability density (3.7) exhibits a sinusoidal behavior, whose

amplitude decreases with K^{-1}. At high temperatures $(K^{-1} > 10^{-2})$ macroscopic order is lost, which is shown in the nonpositive definite vector correlations and an almost constant value for the OPD (limit of dipoles randomly oriented). This loss can be explained as the effect of the geometrical disorder induced by the fractal character of clusters. When increasing the temperature, the aggregates are more complex and intricate, and the geometrical disorder prevails over microscopic order, overriding long-range orientational correlations. The ordering properties of dipolar clusters change continuously with K^{-1} due to variations in the geometrical disorder (fractal character) of the clusters. This fact suggests a continuous dependence of D on the temperature.

In the 3D case we have only analyzed the limit case of zero temperature. As in the preceding case, a low value for the fractal dimension was found, $D = 1.37 \pm 0.03$. In analyzing the orientational correlations, no order is found even at $T = 0$; in 3D space dipoles are randomly distributed in spite of the relaxation process. Surprisingly, however, when analyzing 2D related properties, namely the OPD of the normalized projections of dipoles over the X-Y plane, we recover the sinusoidal behavior typical of 2D clusters (Fig. 12). In view of these results, we can conclude that, although the relaxation mechanism does not produce an apparent macroscopic ordering in the orientation of 3D dipolar clusters, it indeed induces some underlying order, which is revealed by analyzing the correlations of the normalized projections over a plane. Further work must be done in this direction, including the generation of clusters of size greater than those grown in our present simulations.

ACKNOWLEDGMENTS

[1] T. Vicsek, *Fractal Growth Phenomena*, 2nd ed. (World Scientific, Singapore, 1992).
[2] T. A. Witten and L. M. Sander, Phys. Rev. Lett. **47**, 1400 (1981); Phys. Rev. B **27**, 5686 (1983).
[3] D. A. Weitz and M. Oliveria, Phys. Rev. Lett. **52**, 1433 (1984).
[4] P. Meakin, Phys. Rev. Lett. **51**, 1119 (1983).
[5] M. Kolb, R. Botet, and R. Jullien, Phys. Rev. Lett. **51**, 1123 (1983).
[6] G. C. Ansell and E. Dickinson, Chem. Phys. Lett. **122**, 594 (1985).
[7] P. Meakin and M. Muthukumar, J. Chem. Phys. **91**, 3212 (1989).
[8] P. Meakin, J. Colloid. Int. Sci. **134**, 235 (1990).
[9] R. Jullien and M. Kolb, J. Phys. A **17**, L639 (1984).
[10] A. Block, W. von Bloh, and H. J. Schellnhuber, J. Phys. A **24**, L1037 (1991).
[11] A. T. Skjeltorp, Phys. Rev. Lett. **51**, 2306 (1983).
[12] G. Helgesen and A. T. Skjeltorp, J. Appl. Phys. **69**, 8277 (1991).
[13] P. M. Mors, R. Botet, and R. Jullien, J. Phys. A **20**, L975 (1987).
[14] G. Helgesen, A. T. Skjeltorp, P. M. Mors, R. Botet, and R. Jullien, Phys. Rev. Lett. **61**, 1736 (1988).
[15] K. Binder, *Monte-Carlo Methods in Statistical Physics* (Springer, Berlin, 1986).
[16] A. B. Eriksson and M. Jonson, Phys. Rev. B **40**, 884 (1989).
[17] S. Tolman and P. Meakin, Phys. Rev. A **40**, 428 (1989).
[18] I. Yekutieli, B. B. Mandelbrot, and H. Kaufman, J. Phys. A **27**, 275 (1994).
[19] P. Meakin, J. Phys. A **18**, L661 (1985).